Dynamics of three-Airy beams carrying optical vortices

Yana V. Izdebskaya,[1,*] Ting-Hua Lu,[2] Dragomir N. Neshev,[1] and Anton S. Desyatnikov[1]

[1]Nonlinear Physics Centre, Research School of Physics and Engineering, The Australian National University, Canberra, 0200 ACT, Australia

[2]Department of Physics, National Taiwan Normal University, Taipei 11677, Taiwan

*Corresponding author: yana.izdebskaya@anu.edu.au

Received 18 November 2013; revised 4 February 2014; accepted 9 February 2014; posted 18 February 2014 (Doc. ID 201514); published 21 March 2014

We study numerically and demonstrate experimentally a novel type of singular optical beams formed by the phase imprinting of an optical vortex into the structure of the three-Airy beams. In contrast to a vortex-free product of three Airy beams, in this type of singular-Airy beam, the vortex in the beam axis causes a twist in the beam transverse intensity profile with propagation. Such a new type of singular beams appears especially attractive for applications in optical micromanipulation.

OCIS codes: (090.1970) Diffractive optics; (080.4865) Optical vortices; (260.6042) Singular optics.
http://dx.doi.org/10.1364/AO.53.00B248

1. Introduction

In recent years, we have seen a continued interest in new applications of the so-called "structured" light, meaning laser beams with spatially varying intensity, phase, or polarization [1,2]. Traditionally, the complex spatial structure of an optical beam is associated with the presence of phase singularities [3] or optical vortices, actively studied in linear [4,5] and nonlinear [6] singular optics. One of the most developed applications of structured light is optical tweezers, able to efficiently trap and manipulate small particles [7] and already available commercially. Optical micromanipulation with structured light stimulated the development of optical tweezers based on vortex beams [8,9], bottle beams [10,11], and even self-propelled beams [12], similar to spiraling beams studied earlier [13,14].

Special attention has been devoted to the use of Airy beams [15–19] due to their unique properties, namely that they are nondiffracting within a diffraction-free zone, undergo self-acceleration during propagation, and display shape recovery after passing through obstacles. Nonspreading Airy wavepackets were studied by Berry and Balazs in 1979 [20], but the concept of nondiffracting self-bending optical beams was first introduced and experimentally demonstrated by Siviloglou *et al.* only recently [21]. Quickly after this seminal work, the field of Airy beams has experienced a rapid development with Airy beam particle sorting [16], second-harmonic generation [22], and curved plasma channel generation [23]. Airy plasmons polaritons [24–26], nonparaxial analogs of Airy beams [27–30], and even electron Airy beams [31] have also been recently demonstrated.

The combination of the two highly nontrivial features, namely optical vortices and self-accelerating Airy beam-shapes, also attracted significant attention. The concept of "self-accelerating vortices" [32] was developed in theory [33] and experiment [34], with many recent results [35,36], including dynamics in uniaxial [37] and nonlinear [38] media, as well as particle manipulation with vortex Airy beams [39].

Recently, the so-called three-Airy beams have been theoretically proposed by Abramochkin and Razueva [40], and they were experimentally observed in linear and nonlinear regimes [41]. Such two-dimensional beams appear attractive for applications in light trapping due to their complex three-dimensional distribution of intensity pattern, allowing for the construction of novel types of optical tweezers for the trapping of multiple dielectric particles [42]. The three-Airy beams are constructed by a product of three Airy wave functions [40], with the envelope of the monochromatic electric field $\mathcal{E}$ which depends on transverse coordinates $\mathbf{r} = \{x, y\}$

$$\mathcal{E}(\mathbf{r};b,c)=\mathrm{Ai}\left(b\frac{x\sqrt{3}-y}{2}+c\right)\times\mathrm{Ai}\left(b\frac{-x\sqrt{3}-y}{2}+c\right)\times\mathrm{Ai}(by+c),\quad(1)$$

where b defines the transverse scale, while the displacement parameter c defines the structure of the beam. The two choices of this parameter are (i) $c=3^{-2/3}a_3'$, with $a_3'=-4.82$, and (ii) $c=3^{-2/3}a_3$, with $a_3=-5.52$. According to the theory [40], these two examples represent two qualitatively different structures: for the first choice of parameter c these beams have a central intensity peak, while the second choice results in a central dark core resembling a dark core of optical vortices but without the vortex phase singularity.

While the class of beams described by Eq. (1) is quite generic, it lacks the possibility for imprinting a phase singularity in the beam center such as explicit appearance of a topological charge in, e.g., family of Laguerre–Gaussian beams. Such singularity will dramatically change the propagation dynamics of the beam and will allow for the realization of twisted-type optical traps and particle manipulators. However, to the best of our knowledge, the properties of singular beams formed by a product of three Airy beams with vortex singularity imprinted in momentum space have not been studied to date. Here, we report on the first experimental observation of such novel types of singular beams. We study the difference between such beams and the "vortex-free" original three-Airy beams [Eq. (1)] and describe how the imprinted vortex phase dramatically changes the beam propagation behavior. In particular, we observe that singular three-Airy beams are propagated with the twisted intensity distribution and form multiple phase singularities evolving with propagation. Furthermore, the autofocusing properties of such beams are investigated, exploring the capability for using vortex Airy beams in optical trapping and micromachining applications.

First, for the two types of three-Airy beams introduced above, we study experimentally the dynamics of vortex-free three-Airy beams as defined by Abramochkin and Razueva [40] and find an excellent match to previous experiments. We then compare these results with the dynamics of the singular three-Airy beams, namely we imprint in the Fourier space the vortex phase structure in two types of three-Airy beams [Eq. (1)] as follows:

$$\Psi_0\equiv\Psi(k_x,k_y)=(k_x+imk_y)\cdot\mathcal{F}(\mathcal{E}(x,y;b,c))=(k_x+imk_y)\mathrm{Ai}\left(3^{2/3}c+2\frac{k_x^2+k_y^2}{3^{4/3}b^2}\right)\times\exp\left(-2i\frac{3k_x^2-k_y^2}{27b^3}k_y\right),\quad(2)$$

where the Fourier transform is $\mathcal{F}(f)=(1/2\pi)\int\int f(x,y)e^{-ixk_x-iyk_y}\mathrm{d}x\mathrm{d}y$, with spatial frequencies (k_x,k_y), and the vortex charge is $m=\pm1$. In the following, we will use the topological charge $m=-1$ to match our experiments.

We model the propagation of singular three-Airy beams by solving numerically the paraxial wave equation in free space using the split-step beam propagation method

$$2ik_0\partial_z\psi+\partial_{xx}^2\psi+\partial_{yy}^2\psi=0,\quad(3)$$

which governs the evolution of the electric field envelope $\psi(x,y,z)$ of the laser beam. Here, the wavevector $k_0=2\pi/\lambda$, and as an initial condition we take the function $\psi(x,y,0)=\mathcal{F}^{-1}(\Psi_0)$.

2. Experimental Arrangements

In our experiments, we employ a spatial light modulator (SLM) in order to encode the correct field distribution. As such, we prepare holograms encoding the required field as a phase-only mask [43] with the transmission

$$T(k_x,k_y)=\exp\left(i\frac{|\Psi_0|\arg\Psi_0}{\max(|\Psi_0|)}+iKk_x\right),\quad(4)$$

where the additional tilt K is used to separate the diffraction orders. In the following, we use $K=30$ in the square window of 768 pixels with width $15b$ and choose the scale parameter $b=1$.

Figure 1 shows a sketch of our experimental setup. A linearly polarized laser beam (cw, $\lambda=532$ nm) with an output Gaussian profile of full width at half-maximum 1.2 mm was expanded using a dual lens telescope (L1 and L2) to a size of 15 mm. The expanded Gaussian laser beam is directed at a small angle to a reflective SLM (Hamamatsu X8267M, 1024×768 pixels). Each pixel acts as an electrically controllable phase plate where the total phase shift exceeds 2π radians as a function of the gray level at the cw laser wavelength of 532 nm.

The phase-modulated reflected wavefront is then Fourier transformed by a lens, L3 ($f=500$ mm).

An iris diaphragm was introduced to the beam path to allow for spatial filtering to block all the unwanted diffraction orders. Finally, the intensity distribution of the isolated first diffraction order along the propagation is recorded using a linear CCD camera (2592×1944 pixels). The CCD was

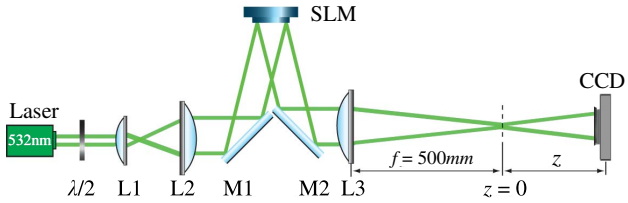

Fig. 1. Experimental setup. $\lambda/2$, half-wavelength plate; L1 and L2, dual lens telescope; M1 and M2, mirrors; SLM, spatial light modulator; L3, Fourier lens; CCD, camera.

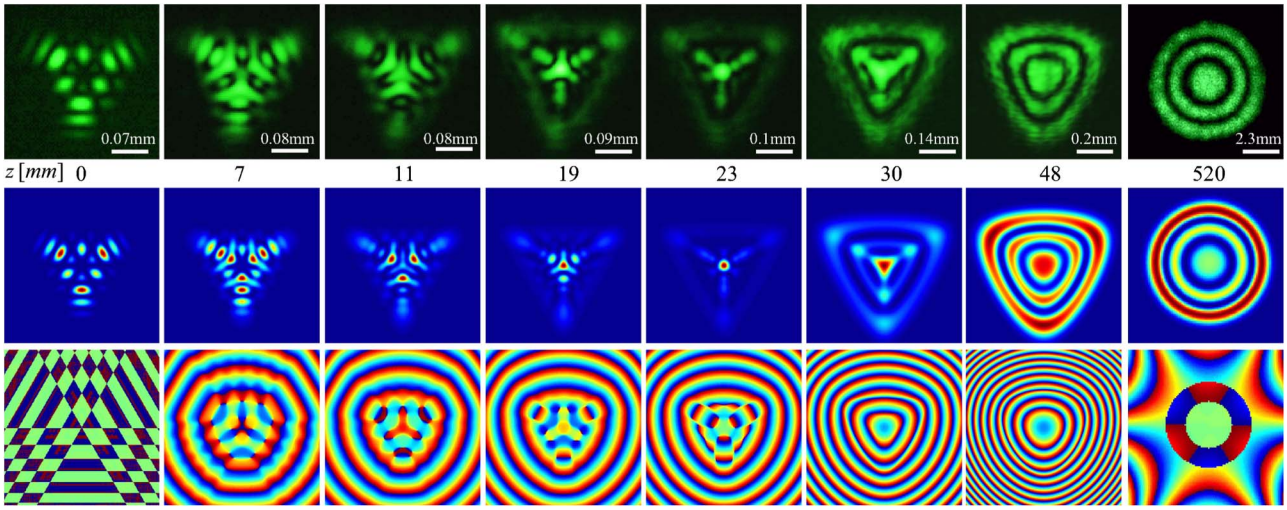

Fig. 2. Propagation of a product of three Airy beams for $c = 3^{-2/3}a'_3$ with $a'_3 = -4.82$ at different propagation distances z: (top row) the experimental results, (middle row) the intensity distribution, and (bottom row) the corresponding phase distribution obtained numerically. The window size in the numerical frames are scaled by $\sqrt{1+z^2}$, as introduced in [40]. Here and in figures below, the intensities in the experimental images (top rows) are scaled from zero (black) to a maximum value (green), the numerical intensities (middle rows) are similar from blue to red, and the phase profiles (bottom rows) are scaled from $-\pi$ (blue) to $+\pi$ (red).

mounted on a translation stage oriented parallel to the propagation axis z. The images were taken at different distances from the focal plane, $z = 0$ to 520 mm.

3. Results and Discussion

We begin our analysis by considering the vortex-free three-Airy beam with parameters $c = 3^{-2/3}a'_3$ and $a'_3 = -4.82$. In Fig. 2 and the following figures, we compare the transverse intensity patterns measured experimentally at various distances z from the focal plane of the Fourier transform system (top rows), with the numerical results for the intensity (middle rows), and phase (bottom rows) spatial distributions.

As is clearly seen in Fig. 2, a triangular pattern of three Airy beams is formed at the focal plane of the lens ($z = 0$) with a diameter ≈0.2 mm. Upon increasing the value of z, the number of lateral side lobes of the beam decreases and a central intensity peak appears at the origin of the triangular beam. It is interesting to note that the observed central intensity peak is a signature of the autofocusing property of the Airy beam at 23 mm, similar to the autofocusing of cylindrically symmetric Airy beams [44]. We define an effective focal distance as the distance between the plane of generation of the Airy beam (the Fourier plane of the lens) and the autofocus position. Most importantly, this distance can be controlled by the initial size and the width of the Airy intensity lobes. Finally, after a long enough propagation $z > 520$ mm, the triangular shape of the three Airy beam transforms into a radially symmetric Airy beam with a few concentric rings and a central main intensity peak. The experimental and numerical results in Fig. 2 are in perfect agreement with the analytical results of [40].

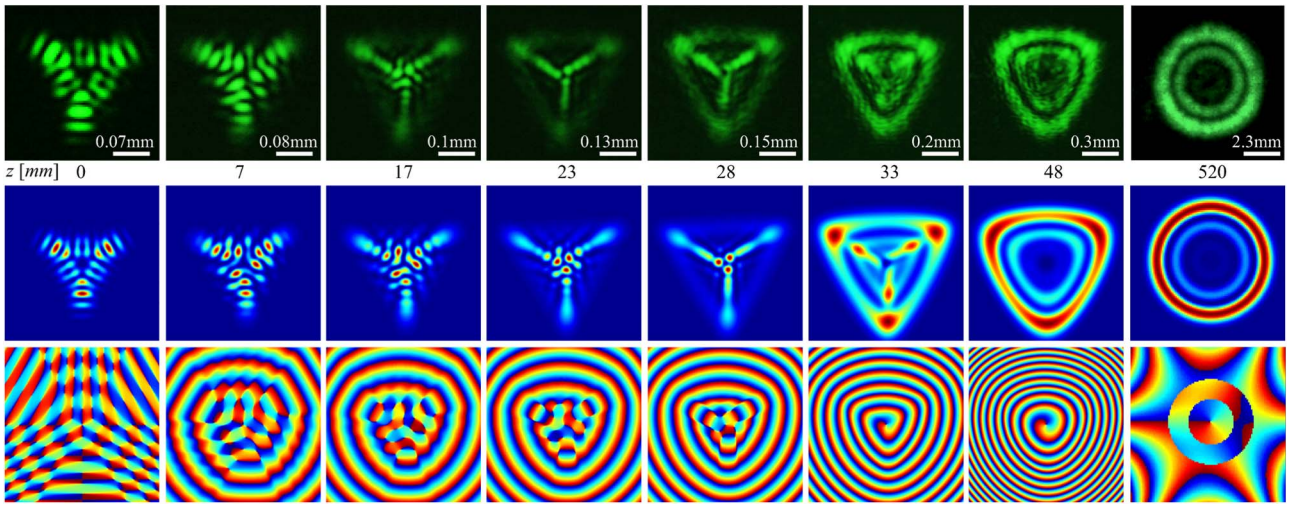

Fig. 3. Same as in Fig. 2 but with the vortex imprinted as in Eq. (2).

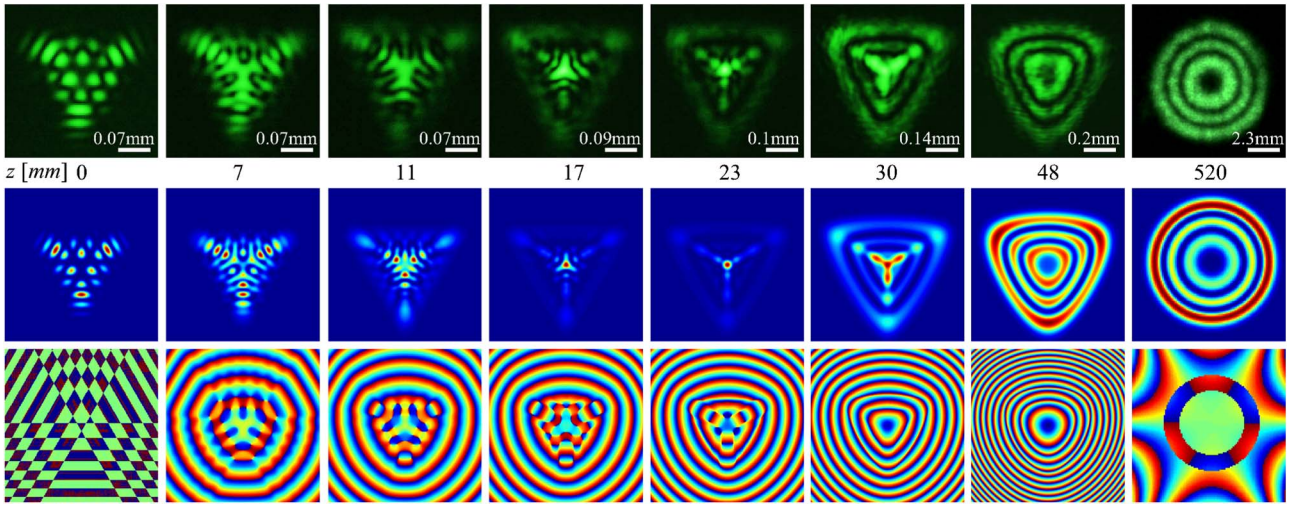

Fig. 4. Same as in Fig. 2 for a vortex-free three-Airy beam with $c = 3^{-2/3}a_3$ and $a_3 = -5.52$.

Our main goal here is to study in detail the behavior of singular three-Airy beams with both choices of parameter sets, similar to the investigation of the product of three-Airy beams. In Fig. 3, the selected cross sections of the normalized beam intensity and the corresponding phases are shown for the singular three-Airy beam of the first type, cf. Fig. 2. In the focal plane of the lens L3 ($z = 0$), a triangular shape of the singular three-Airy beam is formed, which exhibits a minimum intensity in the center, introduced by the imprinted phase singularity. The triangular symmetry remains primary up to $z = 48$ mm. Noticeably, in contrast to the vortex-free three-Airy beams, we find that the intensity profiles of the singular three-Airy beams experience a twist with propagation along the beam axis. Such "propelling" beam evolution is clearly seen in our case in the range $z = 17$–28 mm. Such twist can be explained by the presence of orbital angular momentum of the complex vortex structure that is formed by the imprinted phase singularity and depends on the charge m of the vortex phase in the middle of the beams. For a comprehensive demonstration of the vortex structure, the bottom row in Fig. 4 depicts the numerically obtained phase distributions of the beam. A pure spiral pattern in the phase pictures is observed at $z >$ 33 mm in Fig. 3 (bottom row). For more complicated cases with larger topological charges, the experimental and theoretical analysis employed here can be applied as well. The intensity profiles of such singular three-Airy beams indicate its potential applications in the optical manipulation of micron-sized particles.

Keeping all of the conditions the same as in Fig. 2, we also study the product of three Airy beams for $c = 3^{-2/3}a_3$, with $a_3 = -5.52$. Comparing the intensity and phase distributions of Figs. 2 and 4, we can conclude that this second choice of parameters gives a dark core on the axis, similar to optical vortices but without the vortex phase singularity (see Fig. 4, bottom row).

For comparison, the "propelling" behavior of the intensity distribution of the singular three-Airy beam for $c = 3^{-2/3}a_3$, with $a_3 = -5.52$, are depicted in Fig. 5.

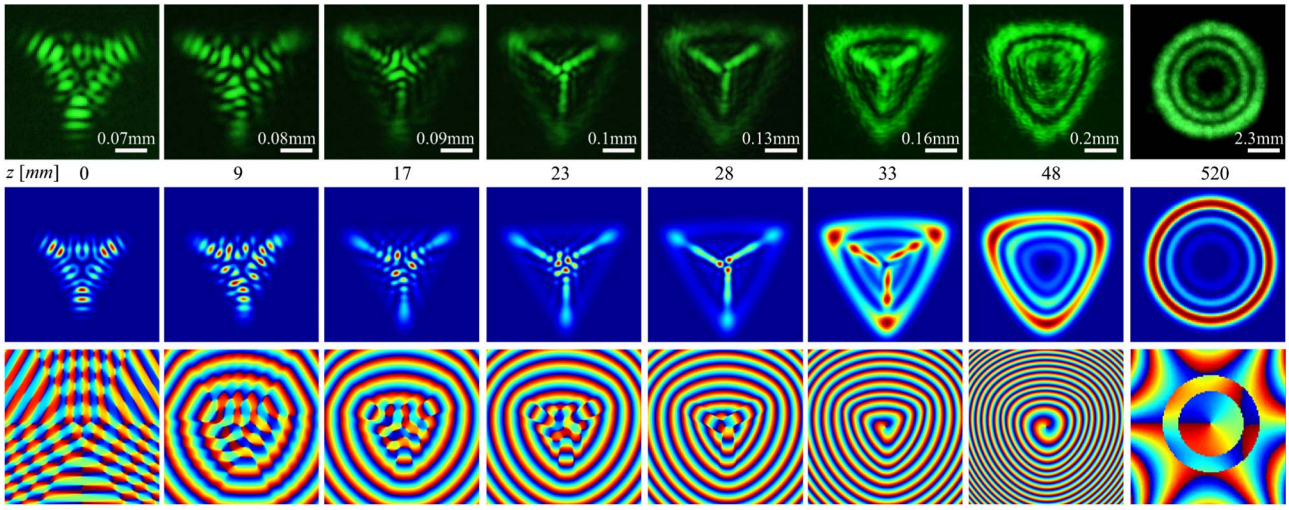

Fig. 5. Same as in Fig. 4 but with a vortex imprinted as in Eq. (2).

The spiral phase distribution of the beam is also shown in Fig. 5, bottom row. The twist of the beam profile is especially evident near the point of beam autofocusing. In contrast to the case of vortex-free three-Airy beams in Fig. 4, here the process of abruptly autofocusing results in the formation of three closely confined light beams at a distance of $z = 28$ mm. All experimental results (Fig. 5, top row) are in excellent agreement with theory.

4. Conclusions

We have studied the propagation of both vortex-free and singular three-Airy beams. The experimental and numerical studies show that the singular beams that formed by imprinting a phase singularity in the Fourier image of the product of three Airy beams results in a twist of the beam intensity distribution along propagation due to the presence of orbital angular momentum and the on-axis optical vortex. A good understanding of the properties of Airy beams is of importance for optical trapping and the interferometric or remote-sensing applications employing them. Due to their unique spatial patterns, such structured laser beams hold great potential for designing new particle trapping schemes with three-dimensional trapping channels and bottle tunnels.

The authors thank Yuri Kivshar for fruitful discussions and acknowledge support by the Australian Research Council.

References

1. *Structured Light and Its Applications*, D. L. Andrews, ed. (Elsevier, 2008).
2. N. M. Litchinitser, "Structured light meets structured matter," Science **337**, 1054–1055 (2012).
3. J. F. Nye and M. V. Berry, "Dislocations in wave trains," Proc. R. Soc. London, Ser. A **336**, 165–190 (1974).
4. M. S. Soskin and M. V. Vasnetsov, "Singular optics," Prog. Opt. **42**, 219–276 (2001).
5. M. R. Dennis, K. O'Holleran, and M. J. Padgett, "Singular optics: optical vortices and polarization singularities," Prog. Opt. **52**, 293–363 (2009).
6. A. S. Desyatnikov, Yu. S. Kivshar, and L. Torner, "Optical vortices and vortex solitons," Prog. Opt. **47**, 291–391 (2005).
7. D. G. Grier, "A revolution in optical manipulation," Nat. Photonics **424**, 810–816 (2003).
8. K. T. Gahagan and G. A. Swartzlander, Jr., "Optical vortex trapping of particles," Opt. Lett. **21**, 827–829 (1996).
9. V. G. Shvedov, A. S. Desyatnikov, A. V. Rode, Y. V. Izdebskaya, W. Krolikowski, and Y. S. Kivshar, "Optical vortex beams for trapping and transport of particles in air," Appl. Phys. A **100**, 327–331 (2010).
10. C. Alpmann, M. Esseling, P. Rose, and C. Denz, "Holographic optical bottle beams," Appl. Phys. Lett. **100**, 111101 (2012).
11. V. G. Shvedov, Y. Izdebskaya, A. V. Rode, A. S. Desyatnikov, W. Krolikowski, and Yu. S. Kivshar, "Generation of optical bottle beams by incoherent white-light vortices," Opt. Express **16**, 20902–20907 (2008).
12. P. Zhang, D. Hernandez, D. Cannan, Y. Hu, S. Fardad, S. Huang, J. C. Chen, D. N. Christodoulides, and Z. Chen, "Trapping and rotating microparticles and bacteria with moiré-based optical propelling beams," Biomed. Opt. Express **3**, 1891–1897 (2012).
13. E. G. Abramochkin and V. G. Volostnikov, "Spiral light beams," Phys. Usp. **47**, 1177–1203 (2004).
14. Y. Izdebskaya, V. Shvedov, and A. Volyar, "Symmetric array of off-axis singular beams: spiral beams and their critical points," J. Opt. Soc. Am. A **25**, 171–181 (2008).
15. M. A. Bandres and J. C. Gutierrez-Vega, "Airy–Gauss beams and their transformation by paraxial optical systems," Opt. Express **15**, 16719–16728 (2007).
16. J. Baumgartl, M. Mazilu, and K. Dholakia, "Optically mediated particle clearing using Airy wavepackets," Nat. Photonics **2**, 675–678 (2008).
17. J. A. Davis, M. J. Mitry, M. A. Bandres, I. Ruiz, K. P. McAuley, and D. M. Cottrell, "Generation of accelerating Airy and accelerating parabolic beams using phase-only patterns," Appl. Opt. **48**, 3170–3176 (2009).
18. S. Barwick, "Accelerating regular polygon beams," Opt. Lett. **35**, 4118–4120 (2010).
19. P. Zhang, J. Prakash, Z. Zhang, M. S. Mills, N. K. Efremidis, D. N. Christodoulides, and Z. Chen, "Trapping and guiding microparticles with morphing autofocusing Airy beams," Opt. Lett. **36**, 2883–2885 (2011).
20. M. V. Berry and N. L. Balazs, "Nonspreading wave packets," Am. J. Phys. **47**, 264–267 (1979).
21. G. A. Siviloglou, J. Broky, A. Dogariu, and D. N. Christodoulides, "Observation of accelerating Airy beams," Phys. Rev. Lett. **99**, 213901 (2007).
22. T. Ellenbogen, N. Voloch-Bloch, A. Ganany-Padowicz, and A. Arie, "Nonlinear generation and manipulation of Airy beams," Nat. Photonics **3**, 395–398 (2009).
23. P. Polynkin, M. Kolesik, J. V. Moloney, G. A. Siviloglou, and D. N. Christodoulides, "Curved plasma channel generation using ultraintense Airy beams," Science **324**, 229–232 (2009).
24. A. Minovich, A. E. Klein, N. Janunts, T. Pertsch, D. N. Neshev, and Y. S. Kivshar, "Generation and near-field imaging of Airy surface plasmons," Phys. Rev. Lett. **107**, 116802 (2011).
25. P. Zhang, S. Wang, Y. Liu, X. Yin, C. Lu, Z. Chen, and X. Zhang, "Plasmonic Airy beams with dynamically controlled trajectories," Opt. Lett. **36**, 3191–3193 (2011).
26. L. Li, T. Li, S. M. Wang, C. Zhang, and S. N. Zhu, "Plasmonic Airy beam generated by in-plane diffraction," Phys. Rev. Lett. **107**, 126804 (2011).
27. A. V. Novitsky and D. V. Novitsky, "Nonparaxial Airy beams: role of evanescent waves," Opt. Lett. **34**, 3430–3432 (2009).
28. P. Zhang, Y. Hu, T. Li, D. Cannan, X. Yin, R. Morandotti, Z. Chen, and X. Zhang, "Nonparaxial Mathieu and Weber accelerating beams," Phys. Rev. Lett. **109**, 193901 (2012).
29. P. Aleahmad, M.-A. Miri, M. S. Mills, I. Kaminer, M. Segev, and D. N. Christodoulides, "Fully vectorial accelerating diffraction-free Helmholtz beams," Phys. Rev. Lett. **109**, 203902 (2012).
30. M. A. Bandres, M. A. Alonso, I. Kaminer, and M. Segev, "Three-dimensional accelerating electromagnetic waves," Opt. Express **21**, 13917–13929 (2013).
31. N. Voloch-Bloch, Y. Lereah, Y. Lilach, A. Gover, and A. Arie, "Generation of electron Airy beams," Nature **494**, 331–335 (2013).
32. M. Mazilu, J. Baumgartl, T. Čižmár, and K. Dholakia, "Accelerating vortices in Airy beams," Proc. SPIE **7430**, 74300C (2009).
33. H. T. Dai, Y. J. Liu, D. Luo, and X. W. Sun, "Propagation dynamics of an optical vortex imposed on an Airy beam," Opt. Lett. **35**, 4075–4077 (2010).
34. H. T. Dai, Y. J. Liu, D. Luo, and X. W. Sun, "Propagation properties of an optical vortex carried by an Airy beam: experimental implementation," Opt. Lett. **36**, 1617–1619 (2011).
35. C. Rosales-Guzmán, M. Mazilu, J. Baumgartl, V. Rodríguez-Fajardo, R. Ramos-García, and K. Dholakia, "Collision of propagating vortices embedded within Airy beams," J. Opt. **15**, 044001 (2013).
36. K. Cheng, X. Zhong, and A. Xiang, "Propagation dynamics, Poynting vector and accelerating vortices of a focused Airy vortex beam," Opt. Laser Technol. **57**, 77–83 (2014).

37. D. Deng, C. Chen, X. Zhao, and H. Li, "Propagation of an Airy vortex beam in uniaxial crystals," Appl. Phys. B **110**, 433–436 (2013).
38. R.-P. Chen, K.-H. Chew, and S. He, "Dynamic control of collapse in a vortex Airy beam," Sci. Rep. **3**, 1406 (2013).
39. J. Zhao, P. Zhang, J. Liu, I. Chremmos, D. Deng, Y. Gao, N. Efremidis, D. N. Christodoulides, and Z. Chen, "Trapping, and guiding microparticles with self-accelerating vortex beams," in *CLEO*, OSA Technical Digest (online) (Optical Society of America, 2013), paper CM1M.6.
40. E. Abramochkin and E. Razueva, "Product of three Airy beams," Opt. Lett. **36**, 3732–3734 (2011).
41. Y. Liang, Z. Ye, D. Song, C. Lou, X. Zhang, J. Xu, and Z. Chen, "Generation of linear and nonlinear propagation of three-Airy beams," Opt. Express **21**, 1615–1622 (2013).
42. J. A. Rodrigo, T. Alieva, E. Abramochkin, and I. Castro, "Shaping of light beams along curves in three dimensions," Opt. Express **21**, 20544–20555 (2013).
43. J. A. Davis, D. M. Cottrell, J. Campos, M. J. Yzuel, and I. Moreno, "Encoding amplitude information onto phase-only filters," Appl. Opt. **38**, 5004–5013 (1999).
44. D. G. Papazoglou, N. K. Efremidis, D. N. Christodoulides, and S. Tzortzakis, "Observation of abruptly autofocusing waves," Opt. Lett. **36**, 1842–1844 (2011).